A peer-reviewed version of this preprint was published in PeerJ on 18 May 2017.

Wang L, Hua Q, Ma Y, Hu G, Qin Y. 2017. Comparative transcriptome analyses of a late-maturing mandarin mutant and its original cultivar reveals gene expression profiling associated with citrus fruit maturation. PeerJ 5:e3343 https://doi.org/10.7717/peerj.3343

Comparative transcriptome analyses of a late-maturing mandarin mutant and its original cultivar reveals gene expression profiling associated with citrus fruit maturation

Wang Lu[1,2], Hua Qingzhu[1], Ma Yuewen[1], Hu Guibing[1], QinYonghua[1]*[1]

[1]State Key Laboratory for Conservation and Utilization of Subtropical Agro-bioresources/Key Laboratory of Biology and Genetic Improvement of Horticultural Crops-South China, Ministry of Agriculture, College of Horticulture, South China Agricultural University, Guangzhou, China.

[2]Yunnan Key Laboratory for Wild Plant Resources/Key Laboratory for Economic Plants and Biotechnology, Kunming Institute of Botany, Chinese Academy of Sciences, Kunming, China.

Abstract

Characteristics of late maturity in fruits are good agronomic traits for extending the harvest period and marketing time. However, underlying molecular basis of the late-maturing mechanism in fruit is largely unknown. In this study, RNA sequencing (RNA-Seq) technology was used to identify differentially expressed genes (DEGs) related to late-maturing characteristics from a late-maturing mutant 'Huawan Wuzishatangju' (HWWZSTJ) (*Citrus reticulata* Blanco) and its original line 'Wuzishatangju' (WZSTJ). A total of approximately 17.0 Gb and 84.2 M paried-end reads were obtained. DEGs were significantly enriched in the pathway of photosynthesis, phenylpropanoid biosynthesis, carotenoid biosynthesis, chlorophyll and abscisic acid (ABA) metabolism. Thirteen candidate transcripts related to chlorophyll metabolism, carotenoid biosynthesis and ABA metabolism were analyzed using real-time quantitative PCR (qPCR) at all fruit maturing stages of HWWZSTJ and WZSTJ. Chlorophyllase (*CLH*) and divinyl reductase (*DVR*) from chlorophyll metabolism, phytoene synthase (*PSY*) and capsanthin/capsorubin synthase (*CCS*) from carotenoid biosynthesis, abscisic acid 8'-hydroxylase (*AB1*) and 9-cis-epoxycarotenoid dioxygenase (*NCED1*) from ABA metabolism were cloned and analyzed. The expression pattern of *NCED1* indicates its role in the late-maturing characteristics of HWWZSTJ. There were 270 consecutive bases missing in HWWZSTJ in comparison with full-length sequences of *NCED1* cDNA from WZSTJ. Those results suggested that *NCED1* might

*Corresponding author. E-mail address: qinyh@scau.edu.cn.

PeerJ Preprints | https://doi.org/10.7287/peerj.preprints.2744v2 | CC BY 4.0 Open Access | rec: 27 Apr 2017, publ: 27 Apr 2017

play an important role in late maturity of HWWZSTJ. This study provides new information of complex process that results in late maturity of *Citrus* fruit at the transcriptional level.

Introduction

Fruit maturity date is an important economic trait and selection of varieties with different harvest time would be advantageous to extend their storage period and market share. Citrus, one of the most important fruit crops, is large-scale commercial production in the tropical and subtropical regions of the world. The total harvested area of citrus exceeds 8.8 million ha, with an annual yield of over 130 million tons in 2015 (FAOSTAT, 2014). Currently, harvest time for most citrus is mainly from November to December resulting in huge market pressure. Therefore, breeding of early- and late-maturing citrus varieties is essential to extend marketing season, meet the needs of consumers and ensure an optimal adaptation to climatic and geographic conditions.

Plant hormones play important roles in the regulation of fruit development and ripening (Kumar et al., 2014). Ethylene is known to be the major hormonal regulator in climacteric fruit ripening. In addition to ethylene, abscisic acid (ABA), auxin, gibberellin (GA) and brassinosteroid are involved in regulating fruit ripening. ABA plays an important role as an inducer along with ethylene signaling for the onset of fruit degreening and carotenoid biosynthesis during development and ripening process in climacteric and non-climacteric fruits (Leng et al., 2009; Sun et al., 2010; Jia et al., 2011; Romero et al., 2012; Soto et al., 2013; Wang et al., 2016). ABA treatment can rapidly induced flavonol and anthocyanin accumulation in berry skins of the *Cabernet Sauvignon* grape suggesting that ABA could stimulate berry ripening and ripening-related gene expression (Koyama et al., 2010). ABA also participated in the regulation of fruit development and ripening of tomato (Zhang et al., 2009b; Sun et al., 2011), cucumber (Wang et al., 2013), strawberry (Jia et al., 2011), bilberry (Karppinen et al., 2013), citrus (Zhang et al., 2014) and grape (Nicolas et al., 2014). Recent studies showed that ABA is a positive regulator of ripening and exogenous ABA application could effectively regulate citrus fruit maturation (Wang et al., 2016). Those results suggest that ABA metabolism plays a crucial role in the regulation of fruit development and ripening. In addition, fruit deterioration and post harvest processes might influence fruit quality and ripening process. However, there were few reports involved in those processes. α-mannosidase (α-Man) and

PeerJ Preprints | https://doi.org/10.7287/peerj.preprints.2744v2 | CC BY 4.0 Open Access | rec: 27 Apr 2017, publ: 27 Apr 2017

β-D-N-acetylhexosaminidase (β-Hex) are the two ripening-specific N-glycan processing enzymes have been proved that their transcripts increased with the in non-climacteric fruit ripening and softening (Ghosh et al., 2011). Genetic results have proved that 9-cis-epoxycarotenoid dioxygenase (NCED) is the key enzyme in ABA metabolism in plants (Liotenberg et al., 1999; Luchi et al., 2001). *NCED1* could initiate ABA biosynthesis at the beginning of fruit ripening in both peach and grape fruits (Zhang et al., 2009a). Silence of *FaNCED1* (encoding a key ABA synthesis enzyme) in strawberry fruit could cause the ABA levels decreased significantly and uncolored fruits and this phenomenon could be rescued by application of exogenous ABA (Jia et al., 2011). Suppression of the expression of *SLNCED1* could result in delay of fruit softening and maturation in tomato (Sun et al., 2012). Overexpression of ABA-response element binding factors (SlAREB1) in tomato could regulate organic acid and sugar contents during tomato fruit development. Higher levels of organic acid, sugar contents and related-gene expression were detected in *SlAREB1*-overexpressing lines in fruit pericarp of mature tomato (Bastías et al., 2014). However, there is little information available about the role of *NCED1* genes in citrus fruit maturation (Zhang et al., 2014).

Bud mutant selection is the most common method for creating novel cultivars in *Citrus*. 'Huawan Wuzishatangju' (HWWZSTJ) mandarin is an excellent cultivar derived from a bud sport of a seedless cultivar 'Wuzishatangju' (WZSTJ). Fruits of HWWZSTJ are mature in late January to early February of the following year, which is approximately 30 d later than WZSTJ (Qin et al., 2013; Qin et al., 2015). Therefore, the late-maturing mutant and its original cultivar are excellent materials to identify and describe the molecular mechanism involved in citrus fruit maturation. In this study, the high efficient RNA-Seq technology was used to identify differentially expressed genes (DEGs) between the late-maturing mutant HWWZSTJ and its original line WZSTJ mandarins. DEGs involved in carotenoid biosynthesis, chlorophyll degradation and ABA metabolism were characterized. The present work could help to reveal the molecular mechanism of late-maturing characteristics of citrus fruit at the transcriptional level.

Materials&Methods

Plant Materials

The late-maturing mutant 'Huawan Wuzishatangju' (HWWZSTJ) (*Citrus reticulata* Blanco) and its original cultivar 'Wuzishatangju' (WZSTJ) were planted in the same orchard in South

PeerJ Preprints | https://doi.org/10.7287/peerj.preprints.2744v2 | CC BY 4.0 Open Access | rec: 27 Apr 2017, publ: 27 Apr 2017

China Agricultural University (23°09′38″N, 113°21′13″E). Ten six-year-old trees of each cultivar were used in this experiment. Peels (including albedo and flavedo fractions) from fifteen uniform-sized fresh fruits were collected on the 275th (color-break stage, i.e. peels turns from green to orange) and 320th (maturing stage) days after flowering (DAF) of HWWZSTJ an 275th (maturing stage) DAF of WZSTJ (**Fig. S1**) in 2012 and pools were named T3, T1 and T2, respectively. Peels from fifteen uniform-sized fresh fruits of HWWZSTJ and WZSTJ were collected on the 255th, 265th, 275th, 285th, 295th, 305th, 315th and 320th DAF in 2012 and used for expression analyses of candidate transcripts associated with chlorophyll, carotenoid biosynthesis and ABA metabolism. All samples were immediately frozen in liquid nitrogen and stored at -80 ℃ until use.

RNA Extraction, Library Construction and RNA-Seq

Total RNA was extracted from peels according to the protocol of the RNAout kit (Tiandz, Beijing, China) and genomic DNA was removed by DNase I (TaKaRa, Dalian, China). RNA quality was analyzed by 1.0% agarose gel and its concentration was quantified by a NanoDrop ND1000 spectrophotometer (NanoDrop Technologies, Wilmington, DE, USA). RNA integrity number (RIN) values (>7.0) were assessed using an Agilent 2100 Bioanalyzer (Agilent Technologies, Santa Clara, CA, USA).

Construction of RNA-Seq libraries was performed by the Biomarker Biotechnology Corporation (Beijing, China). mRNA was enriched and purified with oligo (dT)-rich magnetic beads and then broken into short fragments. The cleaved RNA fragments were reversely transcribed to the first-strand cDNA using random hexamer primers.The second-strand cDNA was synthesized using RNase H and DNA polymerase I. The cDNA fragments were purified, end blunted, 'A' tailed, and adaptor ligated. The distribution sizes of the cDNA in the three libraries were monitored using an Agilent 2100 bioanalyzer. Finally, the three libraries were sequenced using an Illumina HiSeq^{TM} 2500 platform.

Transcriptome Assembly and Annotation

Sequences obtained in this study were annotated in reference to the genome sequence of *Citrus sinensis* (Xu et al., 2013; Wang et al., 2014) using a TopHat program (Trapnell et al., 2009). Functional annotation of the unigenes was performed using BLASTx (Altschul et al., 1997) and

PeerJ Preprints | https://doi.org/10.7287/peerj.preprints.2744v2 | CC BY 4.0 Open Access | rec: 27 Apr 2017, publ: 27 Apr 2017

classified by Swiss-Prot (SWISS-PROT downloaded from European Bioinformatics Institute by Jan., 2013), Clusters of Orthologous Groups of Proteins Database (COG) (Tatusov et al., 2000), Kyoto Encyclopedia of Genes and Genomes Database (KEGG, release 58) (Kanehisa et al., 2004), non-redundant (nr) (Deng et al., 2006) and Gene Ontology (GO) (Harris et al., 2004). The number of mapped and filtered reads for each unigene was calculated and normalized giving the corresponding Reads Per Kilobases per Million reads (RPKM) values. DEGs between the two samples were determined according to a false discovery rate (FDR) threshold of < 0.01, an absolute log2 fold change value of ≥2 and a P-value <0.01.

Gene Validation and Expression Analysis

Data from RNA-Seq were validated using qPCR. All pigment-related (chlorophyll metabolism, carotenoid biosynthesis and ABA metabolism) uni-transcripts were selected to elucidate their expression patterns at all peel coloration stages of HWWZSTJ and WZSTJ with specific primers (**Table S1**). The citrus *actin* gene (accession No. GU911361.1) was used as an internal standard for the normalization of gene expression. Expression levels of all pigment-related uni-transcripts were determined using qPCR in an Applied Biosystems 7500 real-time PCR system (Applied Biosystems, CA, USA). A total of 20.0 μl reaction volume contained 10.0 μl THUNDERBIRD SYBR qPCR Mix (TOYOBO Co., Ltd.), 50×ROX Reference dye, 2.0 μl Primer Mix (5.0 μM), 6.0 μl ddH_2O, and 2.0 μl cDNA (40 ng). The qPCR parameters were: 94 ℃ for 60 s then 40 cycles of 95 ℃ for 15 s, 55 ℃ for 15 s and 72 ℃ for 30 s. All experiments were performed three times with three biological replicates. Relative expression levels of selected transcripts were calculated by the $2^{-\Delta\Delta C}{}_T$ method (Livak & Schmittgen., 2001).

All pigment-related genes (chlorophyll metabolism, carotenoid biosynthesis, ABA metabolism) were cloned using specific primers (**Table S**2). The 20.0 μl of reaction volume contained 2.0 μl 10×PCR buffer, 2.0 μl dNTP (2.0 mM), 0.2 μl of each primer (10 μM), 2.0 μl DNA (100 ng), 0.2 μl LA *Taq* and 13.4 μl ddH_2O. PCR reaction procedure was 94 ℃ for 4 min then 35 cycles of 94 ℃ for 30 s, 55 ℃ for 30 s and 72 ℃ for 2 min, with a final 72 ℃ for 10 min. Nucleotide sequences of the pigment-related genes were analyzed using the National Center for Biotechnology Information (NCBI) Blast program (http://www.ncbi.nlm.nih.gov/BLAST). ORFs were made using the NCBI ORF Finder (http://www.ncbi.nlm.nih.gov/gorf/gorf.html).

PeerJ Preprints | https://doi.org/10.7287/peerj.preprints.2744v2 | CC BY 4.0 Open Access | rec: 27 Apr 2017, publ: 27 Apr 2017

Alignments were done using ClustalX 1.83 and DNAMan software. Phylogenetic analysis of deduced amino acid sequences were performed using MEGA (version 5.0) and the Neighborjoining method with 1,000 bootstrap replicates.

Results

RNA-Seq Analyses

To obtain differentially expressed genes (DEGs) between HWWZSTJ and WZSTJ, three libraries (T1, T2 and T3) were designed for RNA-Seq. As shown in **Table 1**, 26,403,257, 29,163,126, 28,606,868 raw reads were obtained respectively from the three libraries. After removing low-quality bases and reads, a total of approximately 17.0 Gb clean reads were obtained. The GC contents for T1, T2 and T3 were 44.27%, 44.62% and 44.20%, respectively (**Table 1**). The range of most transcripts length was 100-200 bp (**Fig. S2**). Q30 percentage (percentage of sequences with sequencing error rate lower than 0.01%) for each sample was over 90% (**Table 1**).

Table 1 Summary of the sequencing data

Samples	Total reads	Total base	GC content (%)	Q30 (%)
T1	26,403,257	5,332,498,617	44.27	94.11
T2	29,163,126	5,890,197,025	44.62	93.98
T3	28,606,868	5,777,864,876	44.20	93.90

Note: T1, HWWZSTJ (320 DAF); T2, WZSTJ (275 DAF); T3, HWWZSTJ (275 DAF).

A total of 44,664,047, 49,507,338 and 48,492,905 reads were mapped which accounted for 84.58%, 84.88% and 84.76% of the total reads, respectively (**Table 2**). Number of unique mapped reads accounted for 97.14% (T1), 97.25% (T2) and 97.19% (T3) of the total mapped reads compared with 2.86% (T1), 2.75% (T2) and 2.81% (T3) for multiple mapped reads, respectively. Those results suggested that the throughput and sequencing quality was high enough for further analyses.

PeerJ Preprints | https://doi.org/10.7287/peerj.preprints.2744v2 | CC BY 4.0 Open Access | rec: 27 Apr 2017, publ: 27 Apr 2017

Table 2 Summary of the transcriptome annotation compared with the reference genome of *C. Sinensis* (Xu et al., 2013)

Statistics libraries	T1		T2		T3	
	Number	Percentage	Number	Percentage	Number	Percentage
Total reads	52,806,514	100.0%	58,326,252	100.0%	57,213,736	100.0%
Mapped reads	44,664,047	84.58%	49,507,338	84.88%	48,492,905	84.76%
Unique mapped reads	43,386,022	97.14%	48,146,871	97.25%	47,129,445	97.19%
Multiple mapped reads	1,278,025	2.86%	1,360,467	2.75%	1,363,460	2.81%
Pair mapped reads	39,251,294	87.88%	43,459,426	87.78%	42,663,447	87.98%
Single mapped reads	4,574,673	10.24%	5,159,966	10.42%	4,969,429	10.25%

Note: T1, HWWZSTJ (320 DAF); T2, WZSTJ (275 DAF); T3, HWWZSTJ (275 DAF).

Analyses of Differentially Expressed Genes (DEGs)

DEGs were screened by comparison between any two of the three libraries using $p \leq 0.01$ and $2 \leq$ fold changes ≤ 5 as thresholds. A total of 2,687, 3,002 and 1,834 DEGs were obtained between the T1 and T3, T2 and T1, T2 and T3 libraries, respectively (**Fig. 1A**). Among those DEGs, 1,162, 1,567 and 770 were up-regulated and 1,525, 1,435 and 1,064 were down-regulated (**Fig. 1B**). Transcriptional levels of DEGs in HWWZSTJ on 320th DAF were lower than that on 275th DAF in HWWZSTJ suggesting that transcriptional levels of DEGs decreased during fruit maturation in HWWZSTJ (**Fig. 1B**).

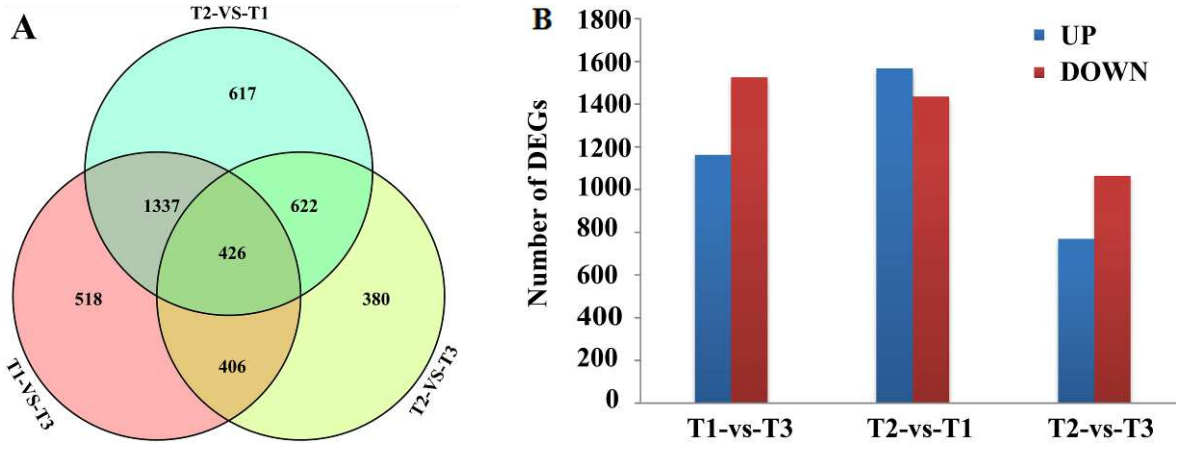

Figure 1 Venn diagram (A) and histogram (B) of DEGs

T1, HWWZSTJ (320 DAF); T2, WZSTJ (275 DAF); T3, HWWZSTJ (275 DAF)

PeerJ Preprints | https://doi.org/10.7287/peerj.preprints.2744v2 | CC BY 4.0 Open Access | rec: 27 Apr 2017, publ: 27 Apr 2017

187 Functional Annotation of Transcripts

188 A total of 299 new transcripts were annotated using five public databases (Nr, Swiss-Prot,
189 KEGG, COG and GO). A summary of the annotations was shown in **Table S3**. Maximum number
190 of annotation of differentially expressed transcripts (2,954) was Nr databases by comparison
191 between T1 and T3, T2 and T1, T2 and T3, followed by GO databases (2,648) (**Table S4**). The
192 differentially expressed transcripts were classified into three categories in GO assignments:
193 cellular component, molecular function and biological process. DEGs between T1 and T3, T2 and
194 T1, T2 and T3 were all significantly enriched in pigmentation, signaling and growth biological
195 processes (**Fig. S3A**). Based on COG classifications, differentially expressed transcripts were
196 divided into 25 different functional groups (**Fig. S3B**). DEGs between any two of the three
197 libraries (T1-VS-T3, T2-VS-T1, T2-VS-T3) were assigned to 91, 100 and 91 KEGG pathways,
198 respectively (**File S1**), and phenylalanine metabolism, porphyrin and chlorophyll metabolism,
199 and flavonoid biosynthesis were the three most significantly enriched biological processes (**Table**
200 **3**).

201

202 **Table 3** Analyses of differentially expressed transcripts based on KEGG pathway

	#	Pathway	DEGs with pathway annotation (283)	All genes with pathway annotation (3516)	p_value	corr_p_value	Pathway ID
	1	Phenylpropanoid biosynthesis	24 (8.48%)	82 (2.33%)	9.58e-09	8.71e-07	ko00940
	2	Photosynthesis	14 (4.95%)	46 (1.31%)	7.90e-06	7.19e-04	ko00195
	3	Plant-pathogen interaction	26 (9.19%)	130 (3.7%)	8.30e-06	7.56e-04	ko04626
	4	Plant hormone signal transduction	31 (10.95%)	180 (5.12%)	2.73e-05	2.49e-03	ko04075
T1	5	Phenylalanine metabolism	17 (6.01%)	72 (2.05%)	3.59e-05	3.26e-03	ko00360
vs	6	Photosynthesis-antenna proteins	7 (2.47%)	15 (0.43%)	7.45e-05	6.78e-03	ko00196
T3	7	Galactose metabolism	10 (3.53%)	45 (1.28%)	2.46e-03	2.23e-01	ko00052
	8	Starch and sucrose metabolism	21 (7.42%)	137 (3.9%)	2.66e-03	2.42e-01	ko00500
	9	Porphyrin and chlorophyll metabolism	8 (2.83%)	37 (1.05%)	7.83e-03	7.12e-01	ko00860

PeerJ Preprints | https://doi.org/10.7287/peerj.preprints.2744v2 | CC BY 4.0 Open Access | rec: 27 Apr 2017, publ: 27 Apr 2017

	10	Amino sugar and nucleotide sugar metabolism	14 (4.95%)	89 (2.53%)	1.06e-02	9.66e-01	ko00520
	1	Photosynthesis	18 (5.17%)	46 (1.31%)	1.1384e-07	1.1384e-05	ko00195
	2	Photosynthesis antenna proteins	10 (2.87%)	15 (0.43%)	1.5234e-07	1.5234e-05	ko00196
	3	Plant-pathogen interaction	32 (9.2%)	130 (3.7%)	5.5471e-07	5.5471e-05	ko04626
	4	Phenylpropanoid biosynthesis	22 (6.32%)	82 (2.33%)	7.9820e-06	7.9820e-04	ko00940
	5	Cyanoamino acid metabolism	9 (2.59%)	22 (0.63%)	1.2713e-04	1.2713e-02	ko00460
T2	6	Biosynthesis of unsaturated fatty acids	9 (2.59%)	29 (0.82%)	1.3656e-03	1.3656e-01	ko01040
vs							
T1	7	Phenylalanine metabolism	16 (4.6%)	72 (2.05%)	1.3850e-03	1.3850e-01	ko00360
	8	Flavonoid biosynthesis	10 (2.87%)	37 (1.05%)	2.3996e-03	2.3996e-01	ko00941
	9	Starch and sucrose metabolism	23 (6.61%)	137 (3.9%)	7.1760e-03	7.1760e-01	ko00500
	10	Stilbenoid, diarylheptanoid and gingerol biosynthesis	5 (1.44%)	14 (0.4%)	8.6944e-03	8.6944e-01	ko00945
	1	Photosynthesis	26 (10.48%)	46 (1.31%)	5.1027e-19	4.6434e-17	ko00195
	2	Photosynthesis-antenna proteins	11 (4.44%)	15 (0.43%)	1.8431e-10	1.6772e-08	ko00196
	3	Phenylpropanoid biosynthesis	24 (9.68%)	82 (2.33%)	6.3286e-10	5.7590e-08	ko00940
	4	Phenylalanine metabolism	16 (6.45%)	72 (2.05%)	2.6448e-05	2.4068e-03	ko00360
	5	Nitrogen metabolism	9 (3.63%)	32 (0.91%)	2.4845e-04	2.2609e-02	ko00910
	6	Flavone and flavonol biosynthesis	6 (2.42%)	15 (0.43%)	3.3744e-04	3.0707e-02	ko00944
T2	7	Cyanoamino acid metabolism	7 (2.82%)	22 (0.63%)	5.4299e-04	4.9412e-02	ko00460
vs							
T3	8	Stilbenoid, diarylheptanoid and gingerol biosynthesis	5 (2.02%)	14 (0.4%)	1.9788e-03	1.8007e-01	ko00945
	9	Glyoxylate and dicarboxylate metabolism	7 (2.82%)	28 (0.8%)	2.6144e-03	2.3791e-01	ko00630
	10	Flavonoid biosynthesis	8 (3.23%)	37 (1.05%)	3.5075e-03	3.1918e-01	ko00941
	11	Porphyrin and chlorophyll metabolism	8 (3.23%)	37 (1.05%)	3.5075e-03	3.1918e-01	ko00860
	12	Plant-pathogen interaction	18 (7.26%)	130 (3.7%)	3.9071e-03	3.5554e-01	ko04626

PeerJ Preprints | https://doi.org/10.7287/peerj.preprints.2744v2 | CC BY 4.0 Open Access | rec: 27 Apr 2017, publ: 27 Apr 2017

Verification the Accuracy of the RNA-Seq Data Using qPCR

Twelve DEGs with significant difference from the three libraries were selected for verification of RNA-Seq data by qPCR. Linear regression analysis showed an overall correlation coefficient of 0.828, indicating a good correlation between qPCR results and the transcripts per kilobase million from the RNA-Seq data (Fig. S4).

DEGs Related to Carotenoid Biosynthesis, Chlorophyll and ABA Metabolism

Analyses of the expression data obtained through RNA-Seq revealed that most DEGs were involved in carotenoid biosynthesis, chlorophyll and ABA metabolism. The main transcripts involved in the three pathways were shown in **Table 4** and heatmap were made based on transcripts per kilobase million from the RNA-Seq data (**Fig. 2**). Three transcripts (*Cs8g15480,* Pheophorbide a oxygenase; *Cs5g16830,* Chlorophyllase type 0 and *Cs3g19690,* Chlorophyll synthase) involved in chlorophyll degradation, six transcripts (*Cs3g19770*, Delta-aminolevulinic acid dehydratase; *Cs9g13460*, Magnesium-chelatase subunit H; *Cs2g05100*, Magnesium-chelatase subunit ChlI-1; *Cs7g19710*, Magnesium-protoporphyrin O-methyltransferase; *Cs6g16200*, Magnesium-protoporphyrin IX monomethyl ester [oxidative] cyclase 1 and *Cs1g06850*, Protochlorophyllide reductase A) involved in chlorophyll biosynthesis, five transcripts (*Cs6g15910*, Phytoene synthase; *Orange1.1t02108*, phytoene synthase 2; *Cs6g13340*, Prolycopene isomerase 1; *Cs4g14850*/*Orange1. 1t00772*, Capsanthin/capsorubin synthase and *Orange_new Gene_1755*, Lycopene beta-cyclase) involved in carotenoid biosynthesis and four transcripts (*Cs2g03270*/*Cs5g14370*, 9-cis-epoxycarotenoid dioxygenase 2; *Cs6g01180*, Xanthoxin dehydrogenase; *Cs7g14820*, Carotenoid cleavage dioxygenase 4a and *Cs6g19380*, ABA 8' -hydroxylase) involved in ABA metabolism were obtained (**Fig. 2** and **Table 4**).

PeerJ Preprints | https://doi.org/10.7287/peerj.preprints.2744v2 | CC BY 4.0 Open Access | rec: 27 Apr 2017, publ: 27 Apr 2017

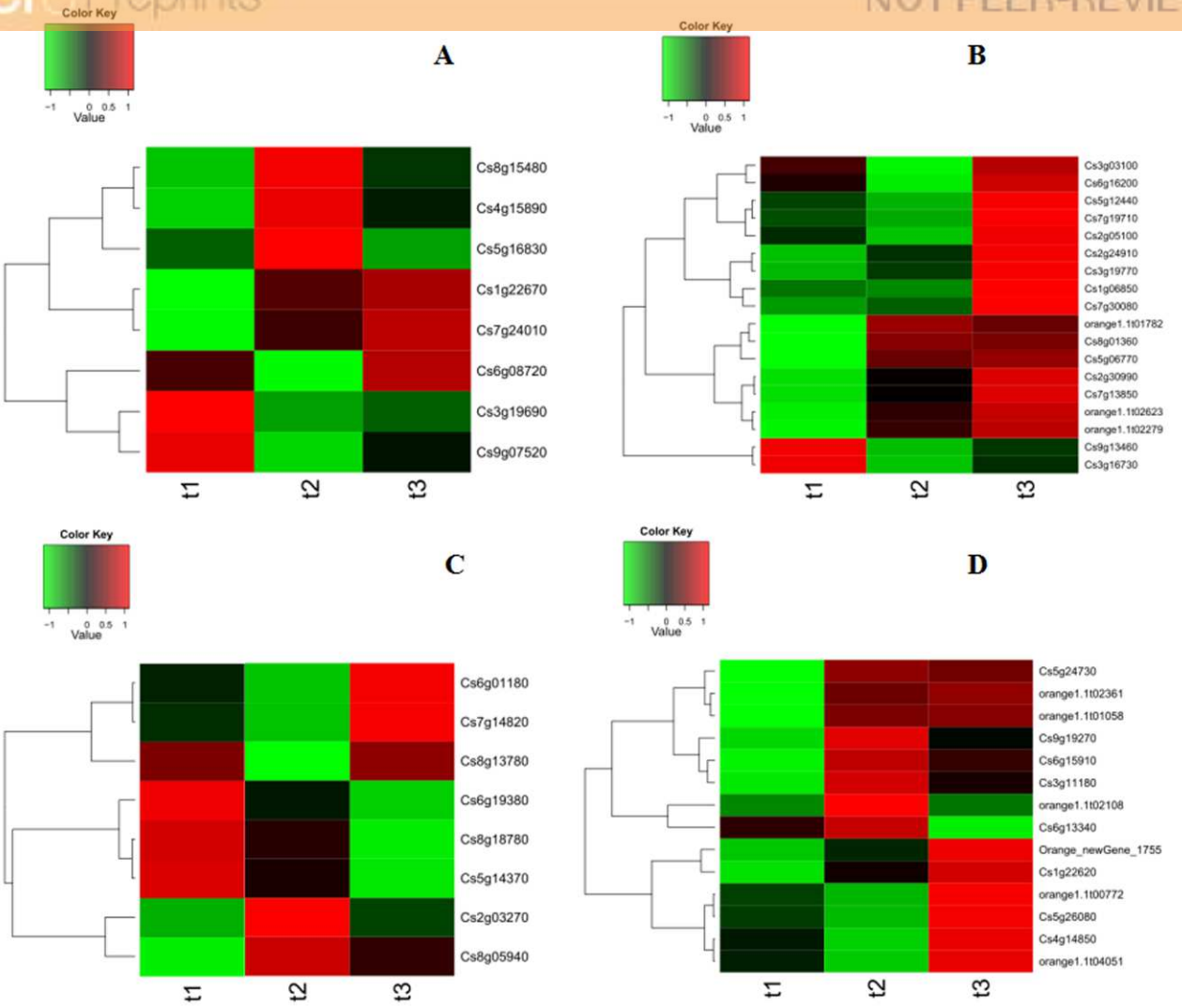

Figure 2 Heatmap of main transcripts from chlorophyll metabolism (A), chlorophyll synthesis (B), carotenoid biosynthesis (C) and ABA metabolism (D)

Table 4 Analyses of transcripts involved in carotenoid biosynthesis, chlorophyll and ABA metabolism

Gene ID	RPKM			Nr-annotation
	T1	T2	T3	
Chlorophyll metabolism				
Cs3g03100	69.88	63.55	72.16	Probable glutamate-tRNA ligase [*Arabidopsis thaliana*]
Cs8g01360	56.22	59.50	59.42	Glutamate-tRNA ligase 1 [*Arabidopsis thaliana*]
Cs3g16730	78.03	66.88	70.76	Glutamyl-tRNA reductase 1 [*Arabidopsis thaliana*]
Orange1.1t02623	89.64	138.40	164.18	Glutamate-1-semialdehyde 2,1-aminomutase 1,

PeerJ Preprints | https://doi.org/10.7287/peerj.preprints.2744v2 | CC BY 4.0 Open Access | rec: 27 Apr 2017, publ: 27 Apr 2017

				Chloroplastic [*Arabidopsis thaliana*]
Cs3g19770	35.03	42.97	62.68	Delta-aminolevulinic acid dehydratase, chloroplastic [*Arabidopsis thaliana*]
Cs7g13850	16.13	23.66	30.83	Porphobilinogen deaminase [*Arabidopsis thaliana*]
Cs5g12440	21.59	19.34	27.86	Uroporphyrinogen decarboxylase 1, chloroplastic
Cs7g30080	53.66	58.13	83.90	Uroporphyrinogen decarboxylase 2, chloroplastic
Orange1.1t02279	37.48	71.77	87.12	Coproporphyrinogen-III oxidase, chloroplastic
Cs5g06770	4.31	6.90	7.22	Oxygen-independent coproporphyrinogen-III oxidase 1
Cs2g24910	21.98	25.25	31.77	Protoporphyrinogen oxidase, chloroplastic/mitochondrial
Orange1.1t01782	35.37	56.42	53.75	Protoporphyrinogen oxidase, chloroplastic
Cs9g13460	44.52	5.36	17.65	Magnesium-chelatase subunit H
Cs2g30990	16.52	19.32	21.84	Magnesium-chelatase 67 kDa subunit
Cs2g05100	118.46	82.35	183.85	Magnesium-chelatase subunit ChlI-1, chloroplastic
Cs7g19710	6.74	3.42	18.65	Magnesium-protoporphyrin O-methyltransferase
Cs6g16200	76.55	14.23	116.31	Magnesium-protoporphyrin IX monomethyl ester [oxidative] cyclase 1
Cs1g06850	22.97	15.00	167.60	Protochlorophyllide reductase A, chloroplastic
Cs5g16830	5.28	29.95	0.81	Chlorophyllase type 0
Cs9g07520	30.05	13.07	20.43	Chlorophyllase type 0
Cs6g08720	57.16	45.38	61.05	Bacteriochlorophyll synthase 34 kDa chain
Cs3g19690	47.34	3.63	10.36	Chlorophyll synthase, putative [*Ricinus communis*]
Cs4g15890	56.44	69.89	61.91	Chlorophyll (ide) b reductase NOL, chloroplastic
Cs7g24010	5.24	11.18	13.54	Chlorophyll (ide) b reductase NOL, chloroplastic
Cs8g15480	64.04	92.78	73.45	Pheophorbide a oxygenase, chloroplastic
Cs1g22670	37.78	73.56	82.11	Red chlorophyll catabolite reductase, chloroplastic
Carotenoid biosynthesis				
Cs6g15910	79.73	216.13	172.64	Phytoene synthase
Orange1.1t02108	30.15	85.62	32.83	PREDICTED: phytoene synthase 2, chloroplastic-like [*Vitis vinifera*]
Orange1.1t02361	50.61	63.09	64.41	Phytoene dehydrogenase, chloroplastic/chromoplastic

PeerJ Preprints | https://doi.org/10.7287/peerj.preprints.2744v2 | CC BY 4.0 Open Access | rec: 27 Apr 2017, publ: 27 Apr 2017

Cs5g24730	47.11	59.11	58.21	15-cis-zeta-carotene isomerase, chloroplastic
Cs3g11180	56.36	81.36	70.96	Phytoene dehydrogenase, chloroplastic/chromoplastic
Cs6g13340	25.39	26.28	23.76	Prolycopene isomerase 1, chloroplastic
Cs4g14850	7.43	5.56	10.07	Capsanthin/capsorubin synthase, chromoplast
Orange1.1t00772	9.33	8.65	11.12	Capsanthin/capsorubin synthase, chromoplast
Orange1.1t01058	38.85	39.93	39.95	Cytochrome P450 97B1, chloroplastic
Cs9g19270	1038.75	1722.54	1359.83	Beta-carotene 3-hydroxylase 1, chloroplastic
Cs1g22620	65.41	82.35	95.98	3-hydroxybenzoate 6-hydroxylase 1
Orange1.1t04051	1.01	0.95	1.10	3-hydroxybenzoate 6-hydroxylase 1
Cs5g26080	11.76	9.88	16.31	Violaxanthin de-epoxidase, chloroplastic
Orange_new Gene_1755	0.45	3.82	9.60	Lycopene beta-cyclase [*Citrus*×*paradisi*]
ABA metabolism				
Cs8g13780	4.47	3.20	4.51	Indole-3-acetaldehyde oxidase
Cs6g01180	46.39	38.09	60.42	Xanthoxin dehydrogenase
Cs2g03270	2.08	67.84	18.90	9-cis-epoxycarotenoid dioxygenase 2 [*Citrus sinensis*]
Cs5g14370	28.65	20.09	8.45	Putative 9-cis-epoxycarotenoid dioxygenase 3 [*Citrus sinensis*]
Cs7g14820	2.18	0.26	5.90	Carotenoid cleavage dioxygenase 4a [*Citrus clementina*]
Cs9g11260	0.00	0.00	0.00	Carotenoid 9,10(9,10')-cleavage dioxygenase 1
Cs6g19380	60.57	30.48	9.86	ABA 8' -hydroxylase [*Citrus sinensis*]
Cs8g05940	2.05	3.80	3.20	Abscisic acid 8'-hydroxylase 1
Cs8g18780	1.10	0.78	0.27	ABA 8' -hydroxylase [*Citrus sinensis*]

According to the result of expression and annotation analyses, thirteen transcripts i.e. *BCHP*, *CRD1*, *CHLM*, *CHLH1*, *HEMFI/HEMF2*, *FC1*, *DVR*, *CAO*, *CLH*, *CCS*, *PSY*, *AB* and *NCED1* associated with chlorophyll metabolism, carotenoid biosynthesis and ABA metabolism were obtained with a Fold Change ≧ 2 and FDR < 0.01 as screening standard (**Table 5**).

PeerJ Preprints | https://doi.org/10.7287/peerj.preprints.2744v2 | CC BY 4.0 Open Access | rec: 27 Apr 2017, publ: 27 Apr 2017

Table 5 Analyses of DEGs associated with carotenoid biosynthesis, chlorophyll and ABA metabolism

Gene ID	Symbols
Chlorophyll metabolism	
Cs5g10740/ Cs2g26780	Geranyl acyl geranyl acyl diphosphate reductase (*BCHP*)
Cs6g16200	Methyl magnesium protoporphyrin IX single cyclase (*CRD1*)
Cs7g19710	Magnesium protoporphyrin IX methyl transferase (*CHLM*)
Cs2g05100/ Cs9g13460	Mg-chelatase subunit D (*CHLD*)/Mg-chelatase subunit H (*CHLH1*)
Orangel1.1t02279	Coproporphyrin oxidative decarboxylase (*HEMFI/HEMF2*)
Cs4g18730	Ferrochelatase (*FC1*)
Cs1g06850	Divinyl reductase (*DVR*)
Cs3g19690	Chlorophyllide a oxygenase (*CAO*)
Cs5g16830	Chlorophyllase (*CLH*)
Carotenoid biosynthesis	
Orange_new Gene_1755	Capsanthin/capsorubin synthase (*CCS*)
Orange1.1t02108/Cs6g15910	Phytoene synthase (*PSY*)
ABA metabolism	
Cs3g23530	Abscisic acid 8'-hydroxylase (*AB*)
Cs5g14370	9-cis-epoxycarotenoid dioxygenase (*NCED1*)

Expression Analyses of Candidate Transcripts

Expression patterns of candidate transcripts associated with chlorophyll metabolism were analyzed between WZSTJ and HWWZSTJ at all fruit maturation stages (**Fig.** 3). Compared with WZSTJ, lower expression levels of *ALAD1* and *CLH* were detected in HWWZSTJ at all fruit maturation stages. Expression of *ALAD1* and *CLH* were increasing before fruit maturation and decreased thereafter in both WZSTJ and HWWZSTJ. The highest expression level of *CLH* was detected on the 295th DAF in HWWZSTJ, which was 20 d later than WZSTJ. Expression levels of *CAO1* and *PAO* in HWWZSTJ was higher than that in WZSTJ. *FC1* showed a decrease trend during fruit maturation of WZSTJ and HWWZSTJ. As for *GluRS*, *CHLH1*, *HEMG* and *CHLM*, they showed irregular expression patterns in WZSTJ and HWWZSTJ **(Fig. 3)**.

PeerJ Preprints | https://doi.org/10.7287/peerj.preprints.2744v2 | CC BY 4.0 Open Access | rec: 27 Apr 2017, publ: 27 Apr 2017

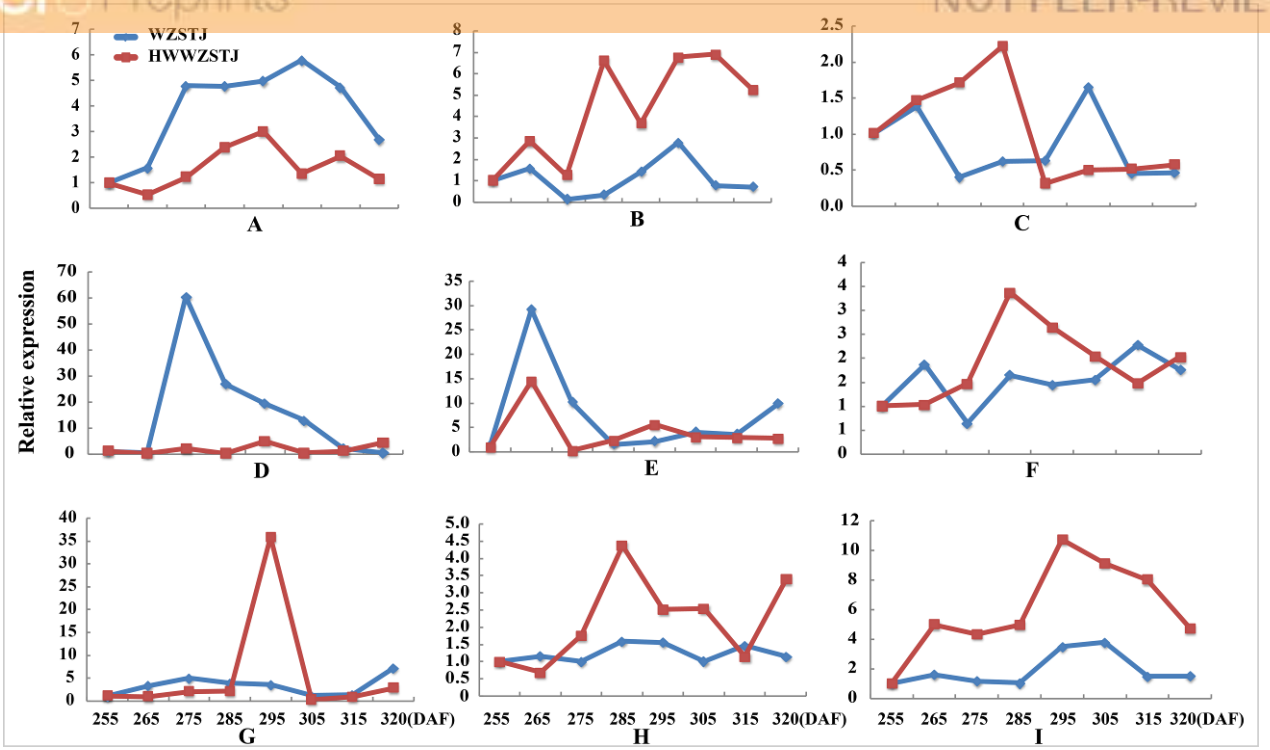

Figure 3 Expression patterns of genes associated with chlorophyll metabolism in WZSTJ and HWWZSTJ at all fruit maturation stages

A, *ALAD1*; B, *CAO1*; C, *CHLM*; D, *CLH*; E, *FC1*; F, *GluRs*; G, *HEMF1*; H, *HEMG*; I, *PAO*

Six carotenoid biosynthesis-related transcripts showed a trend from rise to decline at all fruit maturation stages of WZSTJ and HWWZSTJ (**Fig.** 4). The highest expression level of *CCS* was detected on the 295th DAF in HWWZSTJ which was 20 d later than that of WZSTJ. Expression levels of *PDS1*, *PSY3*, *PSY5*, *PSY6* and *PSY7* in WZSTJ were higher than that of HWWZSTJ. *PDS1* showed an increasing trend during fruit maturing of WZSTJ and HWWZSTJ and reached its maximum expression on the 295th DAF. *PSY5* showed the highest expression levels on the 275th DAF compared to the highest expression levels of *PSY3,* PSY6 and *PSY7* on the 265th DAF in both WZSTJ and HWWZSTJ. Expression levels of *PSY5* were increasing before the 275th DAF and decreased thereafter. *PSY3*, *PSY6* and *PSY7* were up-regulation before the 265th DAF and decreased gradually thereafter **(Fig. 4)**.

PeerJ Preprints | https://doi.org/10.7287/peerj.preprints.2744v2 | CC BY 4.0 Open Access | rec: 27 Apr 2017, publ: 27 Apr 2017

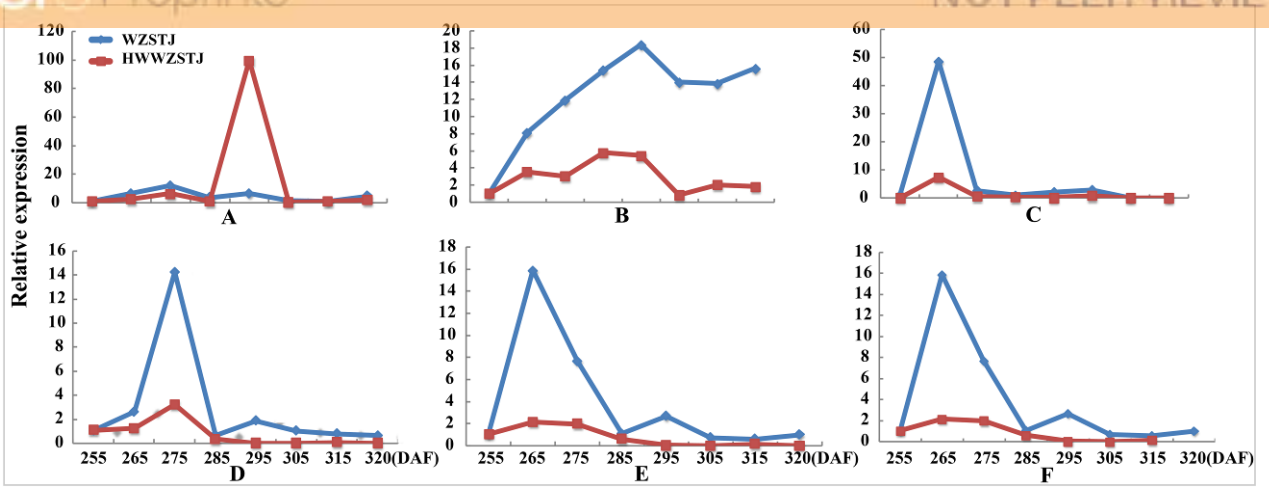

Figure 4 Expression patterns of genes associated with carotenoid biosynthesis in WZSTJ and HWWZSTJ at all fruit maturation stages

A, *CCS*; B, *PDS1*; C, *PSY3*; D, *PSY5*; E, *PSY6*; F, *PSY7*

Expression patterns of two candidate transcripts i.e. *AB1* and *NCED1* related to ABA metabolism were analyzed at all fruit maturation stages of WZSTJ and HWWZSTJ (**Fig.** 5). *AB1* showed a trend from rise to decline during fruit maturation stages of WZSTJ and HWWZSTJ. The highest expression level of *AB1* was obtained on the 295th DAF in HWWZSTJ, which was 20 d later than WZSTJ. Similar expression patterns of *NCED1* were observed before the 295th DAF in HWWZSTJ and WZSTJ (**Fig.** 5). The expression level of *NCED1* in HWWZSTJ was lower than that of WZSTJ during 275th DAF to 305th DAF. The highest expression level of *NCED1* was detected on the 305th DAF of WZSTJ and significantly deceased thereafter (**Fig. 5**). However, the highest expression of *NCED1* was at 295 DAF in HWWZSTJ. Results from expression analyses of candidate genes suggested that *NCED1* might play a leading role in late-maturing characteristics of HWWZSTJ.

PeerJ Preprints | https://doi.org/10.7287/peerj.preprints.2744v2 | CC BY 4.0 Open Access | rec: 27 Apr 2017, publ: 27 Apr 2017

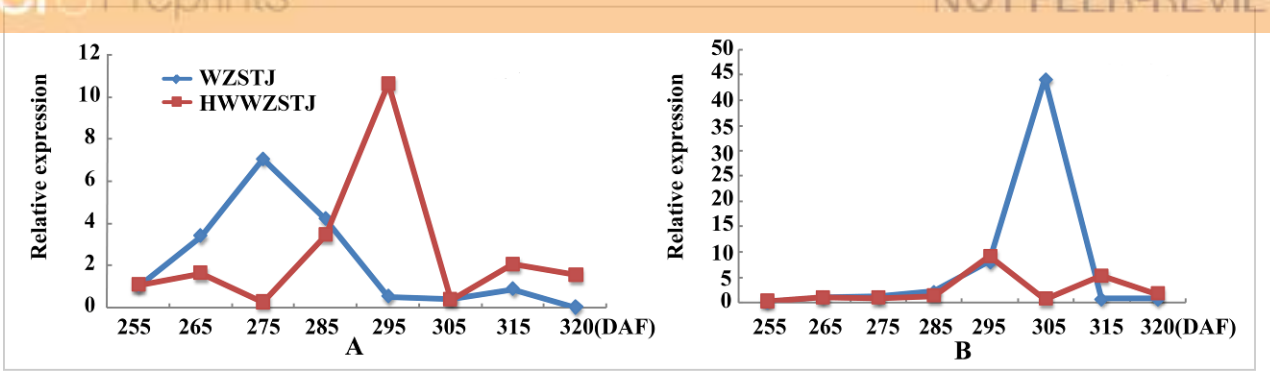

Figure 5 Expression patterns of transcripts associated with ABA metabolism in WZSTJ and HWWZSTJ at all fruit maturation stages

A, *AB1*; B, *NCED1*

Cloning and Phylogenetic Analyses of Candidate Genes

Full-length cDNA sequences of *CLH* and *DVR* from chlorophyll metabolism, *PSY3*, *PSY5*, *PSY6*, *PSY7* and *CCS* from carotenoid biosynthesis, *AB1* and *NCED1* from ABA metabolism were cloned from HWWZSTJ and WZSTJ mandarins. There was one difference in base pair of *CLH*, *PSY3* and *PSY5* cDNA sequences between HWWZSTJ and WZSTJ (**Fig. S5-7**). However, the amino acid sequences of *CLH*, *PSY3* and *PSY5* from HWWZSTJ was 100% identical to that from WZSTJ. There were 4, 6, 4, 3 and 17 bp difference between the sequences of *DVR*, *CCS*, *PSY6*, *PSY7* and *AB1* derived from HWWZSTJ and WZSTJ and this resulted in 2, 3, 3, 1 and 8 differences in the amino acids that would have been incorporated during translation of these transcripts (**Fig. S8-12**). Compared with WZSTJ, there were 270 consecutive bases missing in cDNA sequence of the *NCED1* from HWWZSTJ (**Fig. 6**). Phylogenetic analysis showed that *CLH*, *DVR*, *PSY* and *NCED1* belonged to the same cluster, and their homology in comparison with similar sequences derived from other species is depicted in **Fig. S**13-16**.** Results from sequence analyses suggested that deletion of 270 nucleotides in *NCED1* maybe result in late-maturing characteristics of HWWZSTJ.

PeerJ Preprints | https://doi.org/10.7287/peerj.preprints.2744v2 | CC BY 4.0 Open Access | rec: 27 Apr 2017, publ: 27 Apr 2017

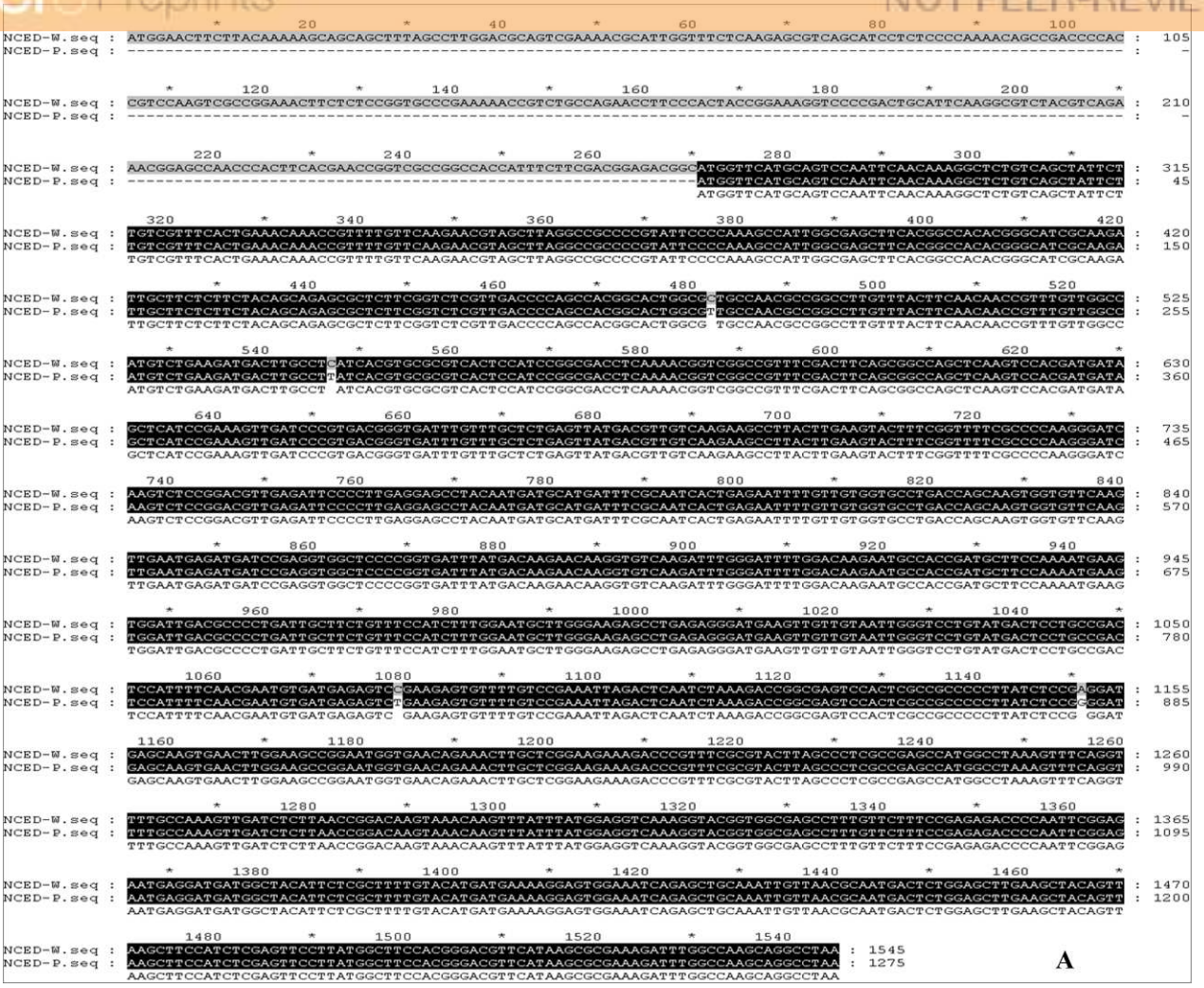

Figure 6 Alignments of cDNA (A) and amino acid (B) sequences of the *NCED1* from HWWZSTJ and WZSTJ W, HWWZSTJ; P, WZSTJ

Discussion

Chlorophyll degradation, carotenoid biosynthesis and ABA metabolism play important roles

PeerJ Preprints | https://doi.org/10.7287/peerj.preprints.2744v2 | CC BY 4.0 Open Access | rec: 27 Apr 2017, publ: 27 Apr 2017

in regulating citrus fruit maturation through a series of related genes or special signal network (Zhang et al., 2014). In this study, RNA-Seq technology was used to screen DEGs between a late-maturing mandarin mutant HWWZSTJ and its wild type WZSTJ during fruit maturation. DEGs between any two of the three libraries were significantly enriched in biological processes such as photosynthesis, phenylpropanoid biosynthesis, carotenoid biosynthesis, chlorophyll metabolism, ABA metabolism, starch and sucrose metabolism (**Table 3**). Thirteen maturing-related genes involved in carotenoid biosynthesis, chlorophyll degradation and ABA metabolism were selected for further analysis.

CLH is the key enzyme catalyzing the first step in the chlorophyll degradation. It can catalyze the hydrolysis of ester bond to yield chlorophyllide and phytol in the chlorophyll breakdown pathway (Jacob-Wilk et al., 1999; Tsuchiya &Takamiya, 1999). Jacob-Wilk et al isolated a CLH encoding an active chlorophyllase enzyme and verified the role of CLH in chlorophyll dephytylation by *in vitro* recombinant enzyme assays. Expression level of *CLH* in Valencia orange peel was low and constitutive and did not significantly increase during fruit development and ripening (Jacob-Wilk et al., 1999). In the present study, a *CLH* was obtained from the transcriptome dataset. No difference was detected in the amino acid sequences of *CLH* between HWWZSTJ and WZSTJ. Expression levels of *CLH* were increasing prior to citrus fruit maturing, decreasing thereafter in both WZSTJ and HWWZSTJ. The highest expression level of *CLH* was detected on the 295th DAF in HWWZSTJ, which was 20 d later than that of WZSTJ (**Fig. 3**). Similar results were also observed in peels of the late-maturing mutant from Fengjie72-1 navel orange (Liu et al., 2006) and Tardivo clementine mandarin (Distefano et al., 2009). Those results suggested that CLH may balance between chlorophyll synthesis and its breakdown (Jacob-Wilk et al., 1999).

Citrus is a complex source of carotenoids with the largest number of carotenoids (Kato, 2004). Carotenoid contents and compositions are main factors that affect peel color of most citrus fruits (Tadeo et al., 2008). PSY is a regulatory enzyme in carotenoid biosynthesis (Welsch et al., 2000). *PSY* is present at low expression level in unripe (green) melon fruit, reaches its highest levels when the fruit turns from green to orange and persists at lower levels during later ripening stages (Karvouni et al., 1995). Liu et al (2006) studied the mechanism underlying the difference between Fengwan (a late-maturing mutant) navel orange and its original cultivar (Fengjie72-1).

PeerJ Preprints | https://doi.org/10.7287/peerj.preprints.2744v2 | CC BY 4.0 Open Access | rec: 27 Apr 2017, publ: 27 Apr 2017

The highest expression levels of some carotenoid biosynthetic enzymes in the peels of the late-maturing mutant occurred 30 d later than that of the original cultivar (Liu et al., 2006). In this work, *PSY* showed a trend from rise to decline at all fruit maturation stages of the late-maturing mutant HWWZSTJ and its original line WZSTJ. The expression levels of *PSY3, PSY5, PSY6* and *PSY7* in HWWZSTJ were lower than that in WZSTJ. These results demonstrated that the mutation in HWWZSTJ influenced the transcriptional activation of *PSY*.

ABA can be considered as a ripening regulator during fruit maturation and ripening. NCED, a key enzyme involved in ABA biosynthesis, plays an important role in fruit ripening of avocado (*Persea americana*) (Chernys and Zeevaart, 2007), orange (*Citrus sinensis*) (Rodrigo et al., 2006), tomato (*Solanum lycopersicum*) (Nitsch et al., 2009; Zhang et al., 2009b), grape (*Vitis vinifera*) and peach (*Prunus persica*) (Zhang et al., 2009a). The *NCED1* were expressed only at the onset stage of ripening in peach and grape, when ABA content became high (Zhang et al., 2009a). Zhang et al. (2014) studied the mechanism of a spontaneous late-maturing mutant of 'Jincheng' sweet orange and its wild type through the comparative analysis. The highest expression of *CsNCED1* was at 215 DAA in WT. In our study, expression levels of *NCED1* increased prior to fruit maturing and decreased significantly thereafter in both HWWZSTJ and WZSTJ. The highest expression level of *NCED1* was detected on the 305th DAF of WT (WZSTJ). Our results were consistent with previous findings that *NCED1* plays the most important role in the ABA biosynthesis pathway during the fruit maturing process (Zhang et al., 2014). Deletion of nucleotides could cause a shift of the reading frame and truncated protein, which can result in natural mutants. Compared with cDNA sequence of *NCED1* from WZSTJ, there were 270 consecutive bases missing in HWWZSTJ (**Fig. 6**). Those results suggested that *NCED1* might play an important role in late-maturing of HWWZSTJ. A high-efficient regeneration system for WZSTJ has been established (Wang et al., 2015) and further study on the role of *NCED1* in citrus is being carried out through genetic engineering.

Conclusion

RNA-Seq technology was used to identify pigment-related genes from a late-maturing mandarin mutant HWWZSTJ and its original cultivar WZSTJ. Thirteen candidate transcripts related to chlorophyll metabolism, carotenoid biosynthesis and ABA metabolism were obtained.

PeerJ Preprints | https://doi.org/10.7287/peerj.preprints.2744v2 | CC BY 4.0 Open Access | rec: 27 Apr 2017, publ: 27 Apr 2017

NCED1, a gene involved in ABA metabolism, is probably involved in the formation of late maturity of HWWZSTJ based on sequence and expression analyses. The present study opens up a new perspective to study the formation of late maturity in citrus fruit.

Acknowledgements

We thank Peng Li, Zixing Ye and Jietang Zhao for help and support with field management and technical assistance.

REFERENCES

Altschul, S.; Madden, T.; Schäffer, A.A.; Zhang, J.; Zhang, Z.; Miller, W.; Lipman, D.J. 1997. Gapped BLAST and PSI-BLAST, A new generation of protein database search programs. *Nucleic Acids Research* 25: 3389-3402.

Bastías, A., López-Climent, M., Valcárcel, M., Rosello, S., Gómez-Cadenas, A., Casaretto, J.A. 2011. Modulation of organic acids and sugar content in tomato fruits by an abscisic acid-regulated transcription factor. *Physiologia Plantarum* 141: 215-226.

Chernys, J.T.; Zeevaart, J.A.D. 2007. Characterization of the 9-cis-epoxycarotenoid dioxygenase gene family and the regulation of abscisic acid biosynthesis in avocado. *Plant Physiology* 124: 343–353.

Deng, Y.Y.; Li, J.Q, Wu, S.F.; Zhu Y.P.; Chen, Y.W.; He, F.C. 2006. Integrated nr database in protein annotation system and its localization. *Computer Engineering* 5: 71–74.

Distefano, G.; Casas, G.; Caruso, M.; Todaro A.; Rapisarda Paolo.; La Malfa S.; Gentile A.; Tribulato E. 2009. Physiological and molecular analysis of the maturation process in fruits of clementine mandarin and one of its late-ripening mutants. *Journal of Agricultural and Food Chemistry* 57: 7974–7982.

FAOSTAT. 2014. *http://faostat.fao.org/site/567/DesktopDefault.aspx?PageID$=$567#ancor.*

Ghosh, S.; Meli, V.S.; Kumar, A.; Thakur, A.; Chakraborty, N.; Chakraborty, S.; Datta, A. 2011. The N-glycan processing enzymes α-mannosidase and β-D-N-acetylhexosaminidase are involved in ripening-associated softening in the non-climacteric fruits of capsicum. Journal of Experimental Botany 62(2): 571–582

Harris, M.A.; Clark, J.; Ireland, A.; Lomax, J.; Ashburner, M.; Foulger, R.; Eilbeck, K.; Lewis, S.; Marshall, B.; Mungall, C.; Richter, J.; Rubin, G.M.; Blake, J.A.; Bult, C.; Dolan, M.; Drabkin, H.; Eppig, J.T.; Hill, D.P.; Ni, L.; Ringwald, M.; Balakrishnan, R.; Cherry, J.M.; Christie, K.R.; Costanzo, M.C.; Dwight, S.S.; Engel, S.; Fisk, D.G.; Hirschman, J.E.; Hong, E.L.; Nash, R.S.; Sethuraman, A.; Theesfeld, C.L.; Botstein, D.; Dolinski, K.; Feierbach, B.; Berardini, T.; Mundodi,

PeerJ Preprints | https://doi.org/10.7287/peerj.preprints.2744v2 | CC BY 4.0 Open Access | rec: 27 Apr 2017, publ: 27 Apr 2017

S.; Rhee, S.Y.; Apweiler, R.; Barrell, D.; Camon, E.; Dimmer, E.; Lee, V.; Chisholm, R.; Gaudet, P.; Kibbe, W.; Kishore, R.; Schwarz, E.M.; Sternberg, P.; Gwinn, M.; Hannick, L.; Wortman, J.; Berriman, M.; Wood, V.; de la Cruz, N.; Tonellato, P.; Jaiswal, P.; Seigfried, T.; White, R. 2004. The Gene Ontology (GO) database and informatics resource. *Nucleic Acids Research* 32: 258–261

Jacob-Wilk, D.; Holland, D.; Goldschmidt, E.E.; Riov, J.; Eyal, Y. 1999. Chlorophyll breakdown by chlorophyllase, Isolation and functional expression of the *Chlase1* gene from ethylene-treated *Citrus* fruit and its regulation during development. *Plant Journal* 20: 653–661.

Jia, H.F.; Chai, Y.M.; Li, C.J; Lu, D.; Luo, J.J.; Qin. L.; Shen, Y.Y. 2011. Abscisic acid plays an important role in the regulation of strawberry fruit ripening. *Plant Physiology* 157 : 188–199.

Kanehisa, M.; Goto, S.; Kawashima, S.; Okuno, Y.; Hattori, M. 2004. The KEGG resource for deciphering the genome. *Nucleic Acids Research* 32: 277–280.

Karppinen, K.; Hirvela, E.; Nevala, T.; Sipari, N.; Suokas, M.; Jaakola, L. 2013. Changes in the abscisic acid levels and related gene expression during fruit development and ripening in bilberry (*Vaccinium myrtillus* L.). *Phytochemistry* 95: 127–134.

Karvouni, Z.; John, I.; Taylor, J.; Watson, C.F.; Turner, A.J.; Grierson, D. 1995. Isolation and characterisation of a melon cDNA clone encoding phytoene synthase. *Plant Molecular Biology* 27: 1153–1162.

Kato, M.; Ikoma, Y.; Matsumoto, H.; Kuniga, T.; Nakajima, N.; Yoshida, T.; Yano, M. 2004. Accumulation of carotenoids and expression of carotenoid biosynthetic genes during maturation in citrus fruit. *Plant Physiology* 134: 824–837.

Koyama, K.; Sadamatsu, K.; Goto-Yamamoto, N. 2010. Abscisic acid stimulated ripening and gene expression in berry skins of the *Cabernet Sauvignon* grape. *Functional & Integrative Genomics* 10: 367-381.

Kumar, R.; Khurana, A.; Sharma, A.K. 2014. Role of plant hormones and their interplay in development and ripening of fleshy fruits. *Journal of Experimental Botany* 65: 4561–4575.

Leng, P.; Zhang, G.L.; Li. X.X.; Wang. L.H.; Zheng, Z.M. 2009. Cloning of 9-cis-epoxycarotenoid dioxygenase (NCED) gene encoding a key enzyme during abscisic acid (ABA) biosynthesis and ABA regulated ethylene production in detached young persimmon calyx. *Chinese Science Bulletin* 54: 2830–2838.

Liu, Y.; Tang, P.; Tao, N.; Xu, Q.; Peng S.A.; Deng X.X.; Xiang K.S.; Huang, R.H. 2006. Fruit coloration

PeerJ Preprints | https://doi.org/10.7287/peerj.preprints.2744v2 | CC BY 4.0 Open Access | rec: 27 Apr 2017, publ: 27 Apr 2017

difference between Fengwan, a late-maturing mutant and its original cultivar Fengjie 72-1 of Navel Orange (*Citrus sinensis* Osbeck). *Zhiwu Shengli yu Fenzi Shengwuxue Xuebao* 32: 31–36.

Liotenberg S, North H, Marion-Poll A. 1999. Molecular biology and regulation of abscisic acid biosynthesis in plants. *Plant Physiology and Biochemistry* 37: 341–350.

Livak, K.J.; Schmittgen, T.D. 2011. Analysis of relative gene expression data using real-time quantitative PCR and the $2^{-\Delta\Delta CT}$ method. *Methods* 25: 402–408.

Luchi S1, Kobayashi M, Taji T, Naramoto M, Seki M, Kato T, Tabata S, Kakubari Y, Yamaguchi-Shinozaki K, Shinozaki K. 2001. Regulation of drought tolerance by gene manipulation of 9-cis-epoxycarotenoid dioxygenase, a key enzyme in abscisic acid biosynthesis in *Arabidopsis*. *Plant Journal* 27: 325–333.

Nicolas, P.; Lecourieux, D.; Kappel, C.; Cluzet, S.; Cramer G.; Delrot S.; Lecourieux F. 2014. The bZIP transcription factor *VvABF2* is an important transcriptional regulator of ABA-dependent grape berry ripening processes. *Plant Physiology* 164: 365–383.

Nitsch, L.; Oplaat, C.; Feron, R.; Ma, Q.; Wolters-Arts, M.; Hedden, P.; Mariani, C.; Vriezen, W.H. 2009. Abscisic acid levels in tomato ovaries are regulated by *LeNCED1* and *SlCYP707A1*. *Planta* 229: 1335–1346.

Qin, Y.H.; Li, G.Y.; Wang, L.; Jaime, A.; Ye, Z.X; Feng, Q.R.; Hu, G.B. 2015. A comparative study between a late-ripening mutant of citrus and its original line in fruit coloration, sugar and acid metabolism at all fruit maturation stage. *Fruits* 70: 5–11.

Qin, Y.H.; Ye, Z.X.; Hu, G.B.; Li, G.Y.; Chen, J.Z.; Lin, S.Q. 2013. 'Huawan Wuzi Shatangju', a late-maturing mandarin cultivar. *Acta Horticulturae Sinica* 40:1411–1412.

Rodrigo, M.J.; Alquezar, B.; Zacarías, L. 2006. Cloning and characterization of two 9-cis-epoxycarotenoid dioxygenase genes, differentially regulated during fruit maturation and under stress conditions, from orange (*Citrus sinensis* L. Osbeck). *Journal of Experimental Botany* 57: 633–643.

Romero, P.; Lafuente, M.T.; Rodrigo, M.J. 2012. The *Citrus* ABA signalosome, identification and transcriptional regulation during sweet orange fruit ripening and leaf dehydration. *Journal of Experimental Botany* 63: 4931-4945.

Soto, A.; Ruiz, K.; Ravaglia, D.; Costa, G.; Torrigiani, P. 2013. ABA may promote or delay peach fruit ripening through modulation of ripening and hormone-related gene expression depending on the developmental stage. *Plant Physiology and Biochemistry* 64: 11–24.

PeerJ Preprints | https://doi.org/10.7287/peerj.preprints.2744v2 | CC BY 4.0 Open Access | rec: 27 Apr 2017, publ: 27 Apr 2017

Sun, L.; Sun, Y.F.; Zhang, M.; Wang, L.; Ren, J.; Cui, M.; Wang, Y.P.; Ji, K.; Li, P.; Li, Q.; Chen, P.; Dai, S.J.; Duan, C.R.; Wu, Y.; Leng, P. 2012. Suppression of 9-cis-Epoxycarotenoid dioxygenase, which encodes a key enzyme in abscisic acid biosynthesis, alters fruit texture in transgenic tomato. *Plant Physiology* 158: 283–298.

Sun, L.; Wang, Y.P.; Chen, P.; Ren, J.; Ji, K.; Li, Q.; Li, P.; Dai, SJ.; Leng, P. 2011. Transcriptional regulation of *SlPYL*, *SlPP2C*, and *SlSnRK2* gene families encoding ABA signal core components during tomato fruit development and drought stress. *Journal of Experimental Botany* 62: 5659–5669.

Sun, L.; Zhang, M.; Ren, J.; Qi, J.; Zhang, G.; Leng P. 2010. Reciprocity between abscisic acid and ethylene at the onset of berry ripening and after harvest. *BMC Plant Biology* 10: 257–268.

Tadeo, F.R.; Cercos, M.; Colmenero-Flores, J.M.; Iglesias, D.J.; Naranjo, M.A.; Rios, G.; Carrera, E.; Ruiz-Rivero, O.; Lliso, I.; Morillon, R.; Ollitrault, P.; Talon, M. 2008. Molecular physiology of development and quality of citrus. *Advances in Botanical Research* 47: 147–223.

Tatusov, R.; Galperin, M.; Natale, D.; Koonin, E.V. 2000. The COG database, A tool for genome-scale analysis of protein functions and evolution. *Nucleic Acids Research* 28: 33–36.

Trapnell, C., Pachter, L., Salzberg, S.L. 2009. TopHat: discovering splice junctions with RNA-Seq. *Bioinformatics* 25: 1105–1111

Tsuchiya, T.; Takamiya, K.I. 1999. Cloning of chlorophyllase, the key enzyme in chlorophyll degradation, finding of a lipase motif and the induction by methyl jasmonate. *Proceedings of the National Academy of Sciences of the United States of America* 96: 15362–15367.

Wang, L.; Li, P.; Su, C.L.; Ma, Y.W.; Yan, L.; Hu, G.B.; Qin, Y.H. 2015. Establishment of a high-efficient regeneration system for Wuzishatangju. *South China Fruits* 44: 48–51.

Wang, X.H., Yin, W., Wu, J.X., Chai, L.J., Yi, H.L. 2016. Effects of exogenous abscisic acid on the expression of citrus fruit ripening-related genes and fruit ripenin. *Scientia Horticulturae* 201: 175–183

Wang J, Chen DJ, Lei Y, Chang JW, Hao BH, Xing F, Li S, Xu Q, Deng XXin, Chen LL. 2014. *Citrus sinensis* annotation project (CAP): a comprehensive database for sweet orange genome. *PLoS ONE* 9: e87723.

Wang, Y.P.; Wang, Y.; Ji, K.; Dai, S.J.; Hu, Y.; Sun, L.; Li, Q.; Chen, P.; Sun, Y.F.; Duan, C.R.; Wu, Y.; Luo, H.; Zhang, D.; Guo, Y.D.; Leng, P. 2013. The role of abscisic acid in regulating cucumber fruit development and ripening and its transcriptional regulation. *Plant Physiology and Biochemistry* 64: 70–79.

Welsch, R.; Beyer, P.; Hugueney, P.; Kleinig, H.; von Lintig, J. 2000. Regulation and activation of phytoene

PeerJ Preprints | https://doi.org/10.7287/peerj.preprints.2744v2 | CC BY 4.0 Open Access | rec: 27 Apr 2017, publ: 27 Apr 2017

497 synthase, a key enzyme in carotenoid biosynthesis, during photomorphogenesis. *Planta* 211: 846–854.

498 **Xu, Q.; Chen, L.L.; Ruan, X.; Chen, D.; Zhu, A.; Chen, C.; Bertrand, D.; Jiao, W.B.; Hao, B.H.; Lyon,**
499 **M.P.; Chen, J.; Gao, S.; Xing, F.; Lan, H.; Chang, J.W.; Ge, X.; Lei, Y.; Hu, Q.; Miao, Y.; Wang, L.;**
500 **Xiao, S.; Biswas, M.K.; Zeng, W.; Guo, F.; Cao, H.; Yang, X.; Xu, X.W.; Cheng, Y.J.; Xu, J.; Liu,**
501 **J.H.; Luo, O.J.; Tang, Z.; Guo, W.W.; Kuang, H.; Zhang, H.Y.; Roose, M.L.; Nagarajan, N.; Deng,**
502 **X.X.; Ruan, Y. 2013.** The draft genome of sweet orange (*Citrus sinensis*). *Nature Genetics* 45: 59–66.

503 **Zhang, M.; Leng, P.; Zhang, G.; Li, X. 2009a.** Cloning and functional analysis of 9-cis-epoxycarotenoid
504 dioxygenase (NCED) genes encoding a key enzyme during abscisic acid biosynthesis from peach and
505 grape fruits. *Journal of Plant Physiology* 166: 1241–1252.

506 **Zhang, M.; Yuan, B.; Leng, P. 2009b.** The role of ABA in triggering ethylene biosynthesis and ripening of
507 tomato fruit. *Journal of Experimental Botany* 60: 1579–1588.

508 **Zhang, Y.; Wang, X.; Wu, J. 2014.** Comparative transcriptome analyses between a spontaneous late-ripening
509 sweet orange mutant and its wild type suggest the functions of ABA, sucrose and JA during citrus fruit
510 ripening. *PLoS ONE* 9: e116056.

511

512

PeerJ Preprints | https://doi.org/10.7287/peerj.preprints.2744v2 | CC BY 4.0 Open Access | rec: 27 Apr 2017, publ: 27 Apr 2017